The connected and leading disconnected diagrams of the hadroniclight-by-light contribution to muon $g-2$

Tom Blum
UConn

Norman Christ
Columbia

Masashi Hayakawa
Nagoya

Taku Izubuchi
BNL/RBRC

Luchang Jin
Columbia

Christoph Lehner
BNL

LATTICE 2016
The 34rd International Symposium on Lattice Field Theory
26 July 2016
Highfield Campus, University of Southampton

Outline

- **Muon Anomalous Magnetic Moment**
- BNL E821 (0.54 ppm) and Standard Model Prediction
- Point Source Photon Method
- Simulations
  - → Muon Leptonic Light by Light
  - → $139\mathrm{MeV}$ Pion $48^3 \times 96$ Lattice
- Finite Volume Effects - QCD box inside QED box
- Long Distance Contribution
- Conclusions and Future Plans

Figure 1. The headstone of Julian Schwinger at Mt Auburn Cemetery in Cambridge, MA.

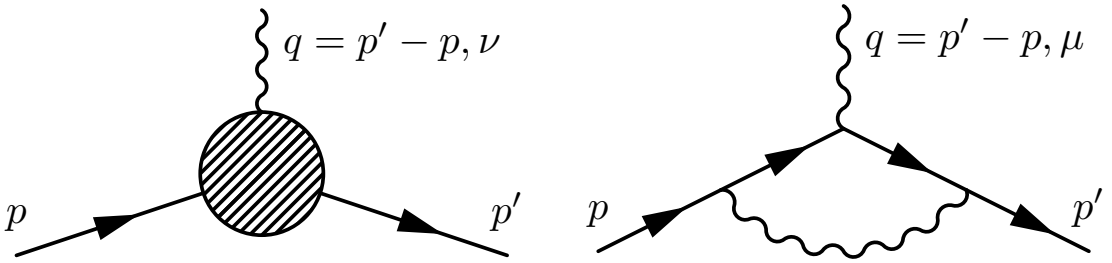

Figure 2. (L) Muon Vertex Function Diagram (R) Schwinger Term Diagram.

$$\begin{aligned}\left\langle \vec{p}', s' \middle| j_\nu\big(\vec{x}_{\rm op}=\vec{0}\big) \middle| \vec{p}, s \right\rangle &= \left\langle \vec{p}', s' \middle| \sum_f q_f \bar{\psi}_f(\vec{x}_{\rm op}=0)\, \gamma_\nu\, \psi_f(\vec{x}_{\rm op}=0) \middle| \vec{p}, s \right\rangle \\ &= -e\, \bar{u}_{s'}(\vec{p}') \left[F_1(q^2)\gamma_\nu + i\frac{F_2(q^2)}{4m}[\gamma_\nu, \gamma_\rho] q_\rho \right] u_s(\vec{p}) \qquad (1)\end{aligned}$$

$$\vec{\mu} = -g\frac{e}{2m}\vec{s} = -(F_1(0) + F_2(0))\,\frac{e}{m}\,\vec{s} \qquad (2)$$

$$F_2(0) = \frac{g-2}{2} \equiv a \qquad (3)$$

Use Euclidean convention by default, the relation is

$$\gamma_4 = (\gamma^0)^M \qquad \boldsymbol{\gamma} = -i\boldsymbol{\gamma}^M \qquad (4)$$

Magentic Moment

Classicaly, magnetic moment is simply

$$\vec{\mu} \;=\; \int \frac{1}{2}\vec{x}\times\vec{j}\,d^3x \tag{5}$$

- This formula is not correct in Quantum Mechanics, because the magnetic moment result from the spin is not included.
- In Quantum Field Thoery, Dirac equation automatically predict fermion spin, so the naive equation is correct again!

$$\langle\vec{\mu}\rangle \;=\; \left\langle\psi\middle|\int \frac{1}{2}\,\vec{x}_{\rm op}\times i\,\vec{j}(\vec{x}_{\rm op})\,d^3x_{\rm op}\middle|\psi\right\rangle \tag{6}$$

- $i\,\vec{j}(\vec{x}_{\rm op})$ is the conventional Minkovski spatial current, because of our γ matrix convention.
- The right hand generate the total magnetic moment for the entire system, including magnetic moment from spin.
- Above formula applies to **normalizable state** with zero total current. Not practical on lattice because it need extremely large volume to evaluate.

$$L \;\gg\; \Delta x_{\rm op}\sim 1/\Delta p \tag{7}$$

Outline

- Muon Anomalous Magnetic Moment
- **BNL E821 (0.54 ppm) and Standard Model Prediction**
- Point Source Photon Method
- Simulations
  - → Muon Leptonic Light by Light
  - → $139\mathrm{MeV}$ Pion $48^3 \times 96$ Lattice
- Finite Volume Effects - QCD box inside QED box
- Long Distance Contribution
- Conclusions and Future Plans

	Value $\pm$ Error	Reference
Experiment (0.54 ppm)	11659208.9 ± 6.3	E821, The $g-2$ Collab. 2006
Standard Model	11659182.8 ± 5.0	Particle Data Group, 2014
Difference (Exp $-$ SM)	26.1 ± 8.0	
HVP LO ($e^+e^- \to$ hadrons)	694.9 ± 4.3	Hagiwara et al. 2011
Hadronic Light by Light	10.5 ± 2.6	Glasgow Consensus, 2007

Table 1. Standard model theory and experiment comparison [in units 10^{-10}]

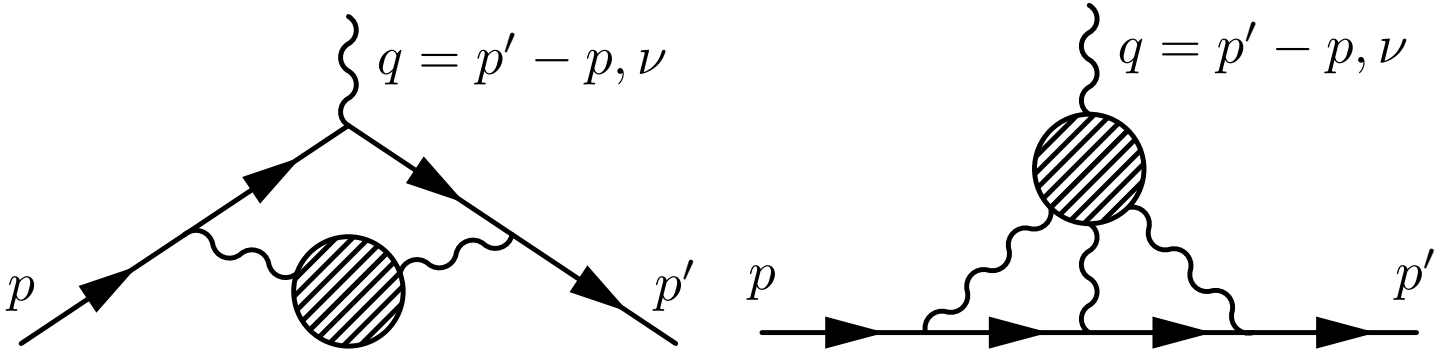

Figure 3. (L) Vaccum polarization diagram. (R) Light by light diagram.

There is 3.3 standard deviations!

Figure 4. 1000 Piece Jigsaw Puzzle - Magnetic Moment. $18.00 from http://eddata.fnal.gov/

Almost 4 times more accurate then the previous experiment.

J-PARC E34 also plans to measure muon $g-2$ with similar precision.

- This subject is started by T. Blum, S. Chowdhury, M. Hayakawa, T. Izubuchi more than 5 years ago. Phys. Rev. Lett. 114, 012001 (2015).
- A series of improvements in methodology is made later by us. Phys.Rev. D93 (2016) no.1, 014503

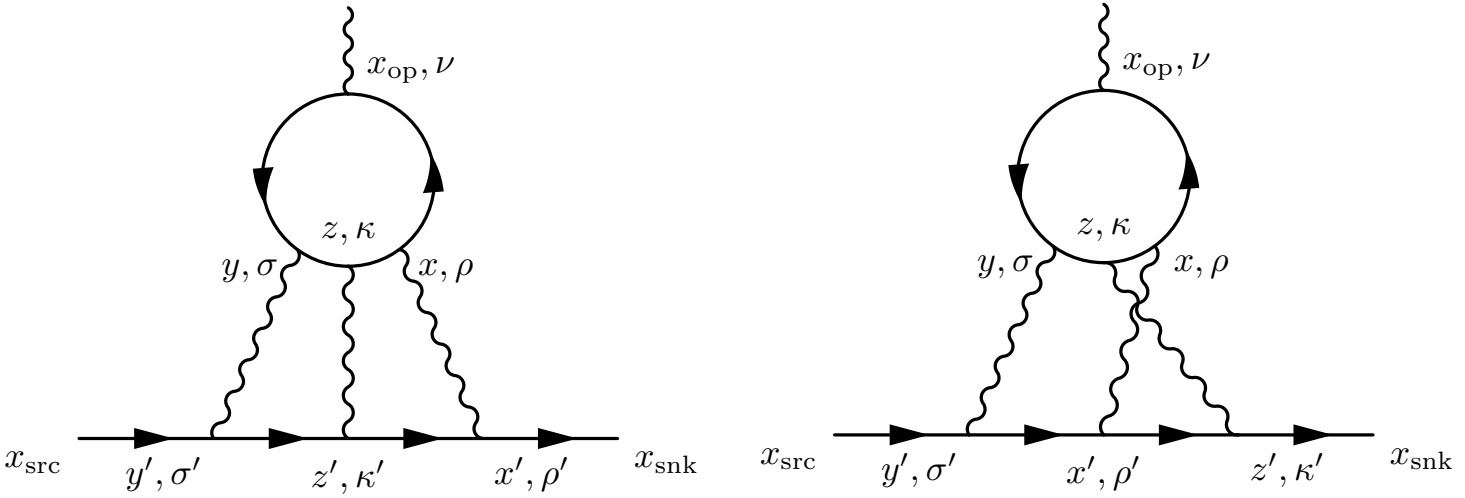

Figure 5. Light by Light diagrams. There are 4 other possible permutations.

Disconnected Diagrams

- One diagram (the biggest diagram below) do not vanish even in the $\mathrm{SU}(3)$ limit.
- We extend the method and computed this leading disconnected diagram as well.

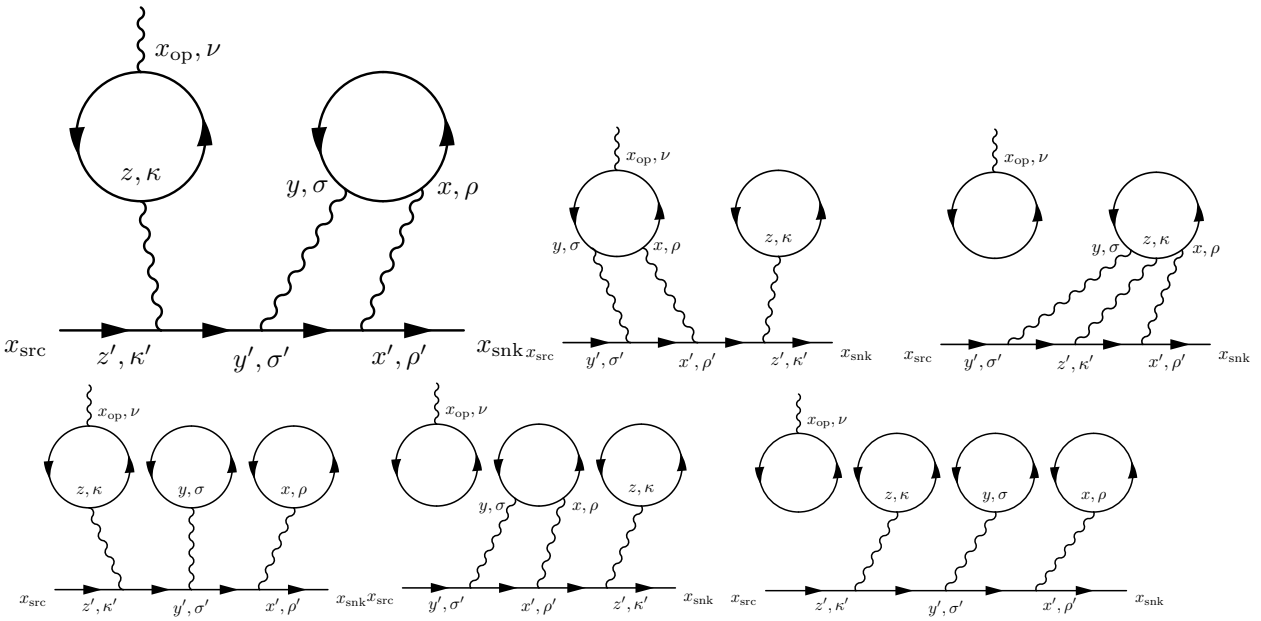

Figure 6. All possible disconnected diagrams. Permutations of the three internal photons are not shown.

- There should be gluons exchange between and within the quark loops, but are not drawn.
- We need to make sure that the loops are connected by gluons by "vacuum" subtraction. So the diagrams are 1-particle irreducible.

Outline

- Muon Anomalous Magnetic Moment
- BNL E821 (0.54 ppm) and Standard Model Prediction
- **Point Source Photon Method**
- Simulations
  - → Muon Leptonic Light by Light
  - → $139\mathrm{MeV}$ Pion $48^3 \times 96$ Lattice
- Finite Volume Effects - QCD box inside QED box
- Long Distance Contribution
- Conclusions and Future Plans

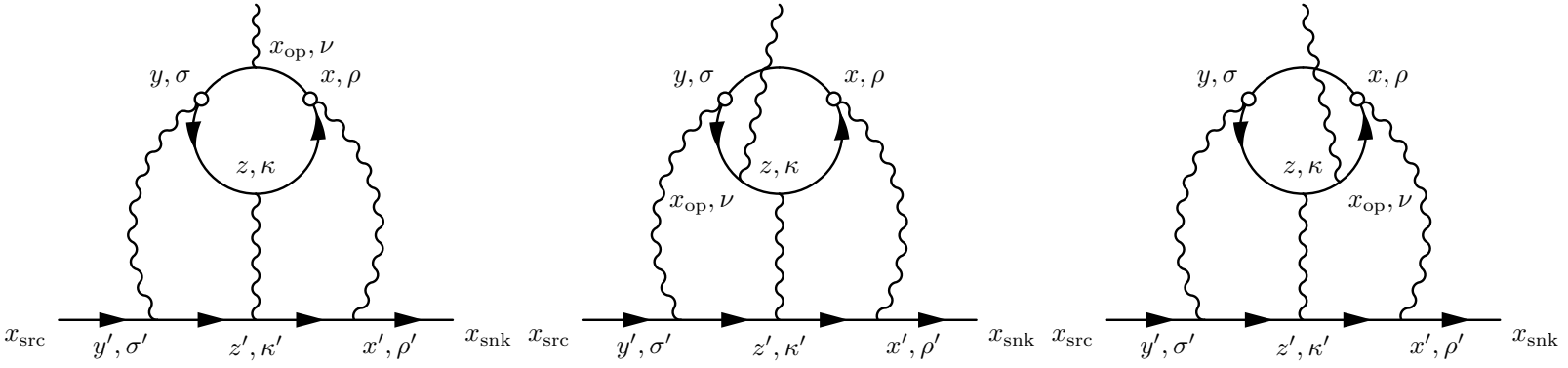

Figure 7. All three different possible insertions for the external photon. 5 other possible permutations of the three internal photons are not shown.

- It is not possible to exactly evaluation the full expression because of too many loops. As a trade off, we can use two point source photons at x and y, which are chosen randomly. It is a very standard 8-dimentional Monte Carlo integral over two space-time points.
- Major contribution comes from the region where x and y are not far separated. Importance sampling is needed. In fact, we can evaluate all possible (upto discrete symmetries) relative positions for distance less than a certain value $r_{\rm max}$, which is normally set to be 5 lattice units.

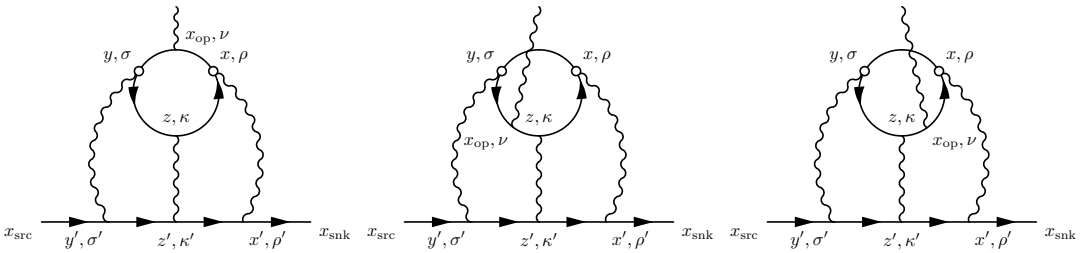

Figure 8. All three different possible insertions for the external photon. 5 other possible permutations of the three internal photons are not shown.

$$\mathcal{F}_\nu^C(x,y,z,x_{\rm op}) = (-ie)^6\,\mathcal{G}_{\rho,\sigma,\kappa}(x,y,z)\sum_{q=u,d,s}(e_q/e)^4 \tag{8}$$

$$\times\ \frac{1}{3}\Big\langle \mathrm{tr}\Big[-\gamma_\rho S_q(x,z)\gamma_\kappa S_q(z,y)\gamma_\sigma S_q(y,x_{\rm op})\gamma_\nu S_q(x_{\rm op},x)\Big] + \text{other 2 permutations}\Big\rangle_{\rm QCD}$$

$$\begin{aligned}&\mathcal{G}_{\rho,\sigma,\kappa}(x,y,z) \\ &= \sum_{x',y',z'} G_{\rho,\rho'}(x,x')G_{\sigma,\sigma'}(y,y')G_{\kappa,\kappa'}(z,z') \\ &\cdot\ e^{m_\mu(t_{\rm snk}-t_{\rm src})}\sum_{\vec{x}_{\rm snk},\vec{x}_{\rm src}}\Big[S_\mu(x_{\rm snk},x')\gamma_{\rho'}S_\mu(x',z')\gamma_{\kappa'}S_\mu(z',y')\gamma_{\sigma'}S_\mu(y',x_{\rm src}) \\ &\quad + S_\mu(x_{\rm snk},z')\gamma_{\kappa'}S_\mu(z',x')\gamma_{\rho'}S_\mu(x',y')\gamma_{\sigma'}S_\mu(y',x_{\rm src}) + \text{other 4 permutations}\Big].\end{aligned} \tag{9}$$

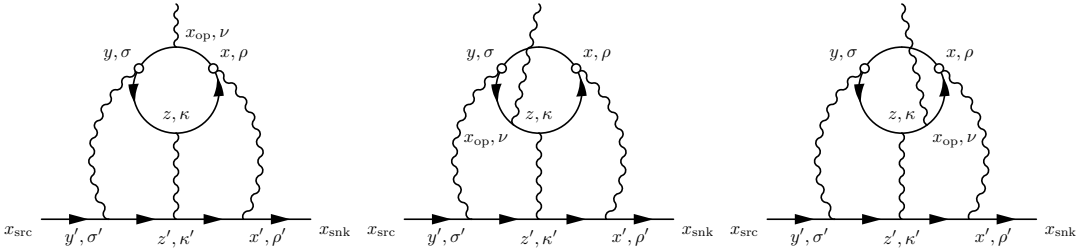

Figure 9. All three different possible insertions for the external photon. 5 other possible permutations of the three internal photons are not shown.

From Phys.Rev. D93 (2016) no.1, 014503

$$\frac{F_2^{\rm cHLbL}(0)}{m}\frac{(\sigma_{s',s})_i}{2} = \sum_{r,\tilde{z}}\sum_{\tilde{x}_{\rm op}}\frac{1}{2}\epsilon_{i,j,k}(\tilde{x}_{\rm op})_j \cdot i\,\bar{u}_{s'}(\vec{0})\,\mathcal{F}_k^C\Big(\frac{r}{2},-\frac{r}{2},\tilde{z},\tilde{x}_{\rm op}\Big)u_s(\vec{0}) \qquad (10)$$

- Recall the definition for $\mathcal{F}_\mu$, we sum all the internal points over the entire space time except we fix $x+y=0$.
- The time coordinate of the current, $(x_{\rm op})_0$ is integrated instead of being held fixed.
- The initial and final muon states are plane waves instead of properly normalized states.

These features allow us to perform the lattice simulation efficiently in finite volume.

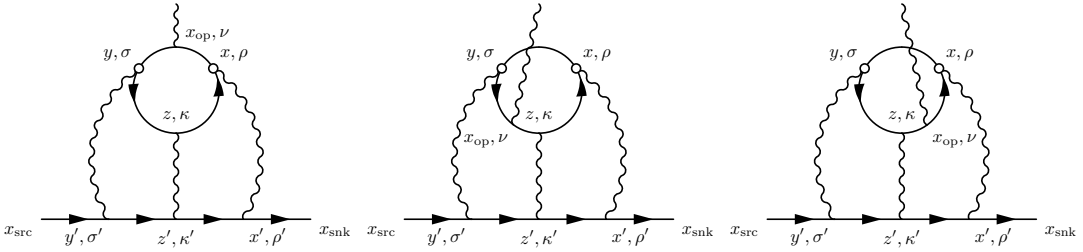

Figure 10. All three different possible insertions for the external photon. 5 other possible permutations of the three internal photons are not shown.

- The points x, y, z are equivalent, we are free to re-label them.
- Since we sum over z, but sample over $r = y - x$. It is beneficial to keep r small, where the fluctuation is small and sampling can be complete.
- So, when we sum over z, we only sum the region where z is far from x, y compare with the distance between x and y.
- This way, we **move** most of the contribution into the small r region, where the fluctuation is small and sampling can be complete.

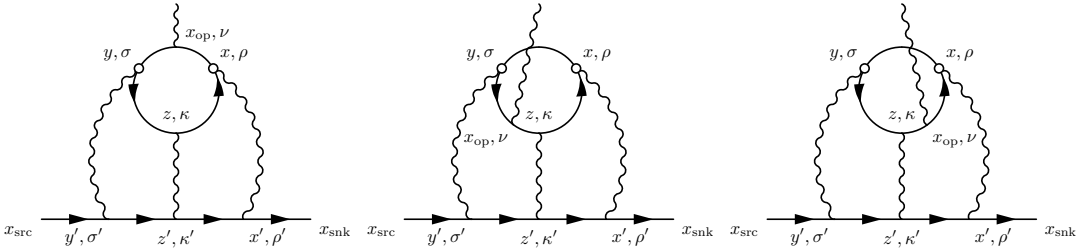

Figure 11. All three different possible insertions for the external photon. 5 other possible permutations of the three internal photons are not shown.

$$= \frac{F_2^{\rm cHLbL}(0)}{m}\frac{(\sigma_{s',s})_i}{2} = \sum_{r,\tilde{z}} \mathfrak{Z}\Big(\frac{r}{2},-\frac{r}{2},\tilde{z}\Big)\sum_{\tilde{x}_{\rm op}} \frac{1}{2}\,\epsilon_{i,j,k}(\tilde{x}_{\rm op})_j \cdot i\,\bar{u}_{s'}(\vec{0})\,\mathcal{F}_k^C\Big(\frac{r}{2},-\frac{r}{2},\tilde{z},\tilde{x}_{\rm op}\Big)u_s(\vec{0}) \tag{11}$$

$$\mathfrak{Z}(x,y,z) = \begin{cases} 3 & \text{if } |x-y|<|x-z| \text{ and } |x-y|<|y-z| \\ 3/2 & \text{if } |x-y|=|x-z|<|y-z| \text{ or } |x-y|=|y-z|<|x-z| \\ 1 & \text{if } |x-y|=|x-z|=|y-z| \\ 0 & \text{otherwise} \end{cases} \tag{12}$$

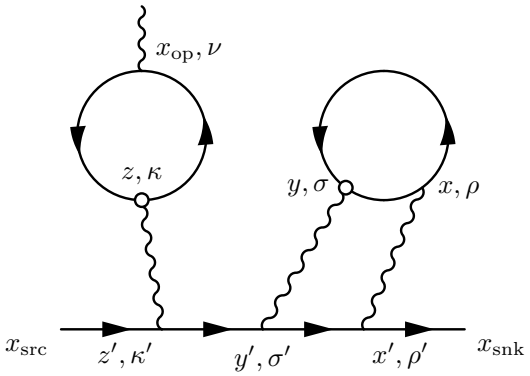

Figure 12. 5 other possible permutations of the three internal photons are not shown.

- We can use two point source photons at y and z, which are chosen randomly. The points $x_{\rm op}$ and x are summed over exactly on lattice.
- Only point source quark propagators are needed. We compute M point source propagators and all M^2 combinations of them are used to perform the stochastic sum over $r = z - y$.

$$\begin{aligned} \mathcal{F}_\nu^D(x,y,z,x_{\rm op}) &= (-ie)^6\,\mathcal{G}_{\rho,\sigma,\kappa}(x,y,z) \\ &\times \left\langle \frac{1}{2}\,\Pi_{\nu,\kappa}(x_{\rm op},z)\,[\Pi_{\rho,\sigma}(x,y) - \Pi^{\rm avg}_{\rho,\sigma}(x-y)] \right\rangle_{\rm QCD} \end{aligned} \tag{13}$$

$$\Pi_{\rho,\sigma}(x,y) = -\sum_q (e_q/e)^2\,{\rm Tr}[\gamma_\rho\,S_q(x,y)\,\gamma_\sigma\,S_q(y,x)]. \tag{14}$$

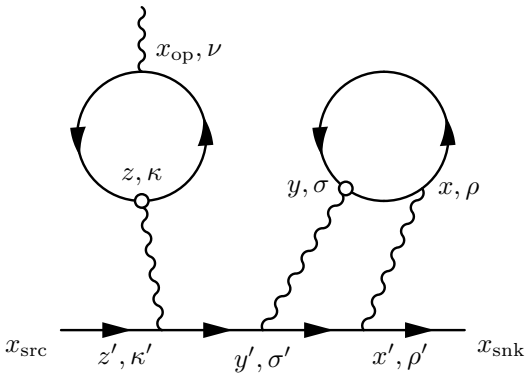

Figure 13. 5 other possible permutations of the three internal photons are not shown.

$$\frac{F_2^{\rm dHLbL}(0)}{m}\frac{(\sigma_{s',s})_i}{2} = \sum_{r,\tilde{x}}\sum_{\tilde{x}_{\rm op}}\frac{1}{2}\epsilon_{i,j,k}(\tilde{x}_{\rm op})_j \cdot i\,\bar{u}_{s'}(\vec{0})\,\mathcal{F}_k^D(\tilde{x},0,r,r+\tilde{x}_{\rm op})u_s(\vec{0}) \tag{15}$$

$$\sum_{\tilde{x}_{\rm op}}\frac{1}{2}\epsilon_{i,j,k}(\tilde{x}_{\rm op})_j\,\langle\Pi_{\rho,\sigma}(\tilde{x}_{\rm op},0)\rangle_{\rm QCD}$$

$$= \sum_{\tilde{x}_{\rm op}}\frac{1}{2}\epsilon_{i,j,k}(-\tilde{x}_{\rm op})_j\,\langle\Pi_{\rho,\sigma}(-\tilde{x}_{\rm op},0)\rangle_{\rm QCD} = 0 \tag{16}$$

- Because of the parity symmetry, the expectation value for the left loop average to zero.
- $[\Pi_{\rho,\sigma}(x,y) - \Pi^{\rm avg}_{\rho,\sigma}(x-y)]$ is only a noise reduction technique. $\Pi^{\rm avg}_{\rho,\sigma}(x-y)$ should remain constant through out the entire calculation.

Outline

- Muon Anomalous Magnetic Moment
- BNL E821 (0.54 ppm) and Standard Model Prediction
- Point Source Photon Method
- **Simulations**
  - → Muon Leptonic Light by Light
  - → $139\mathrm{MeV}$ Pion $48^3 \times 96$ Lattice
- Finite Volume Effects - QCD box inside QED box
- Long Distance Contribution
- Conclusions and Future Plans

- We test our setup by computing **muon leptonic light by light** contribution to muon $g-2$.

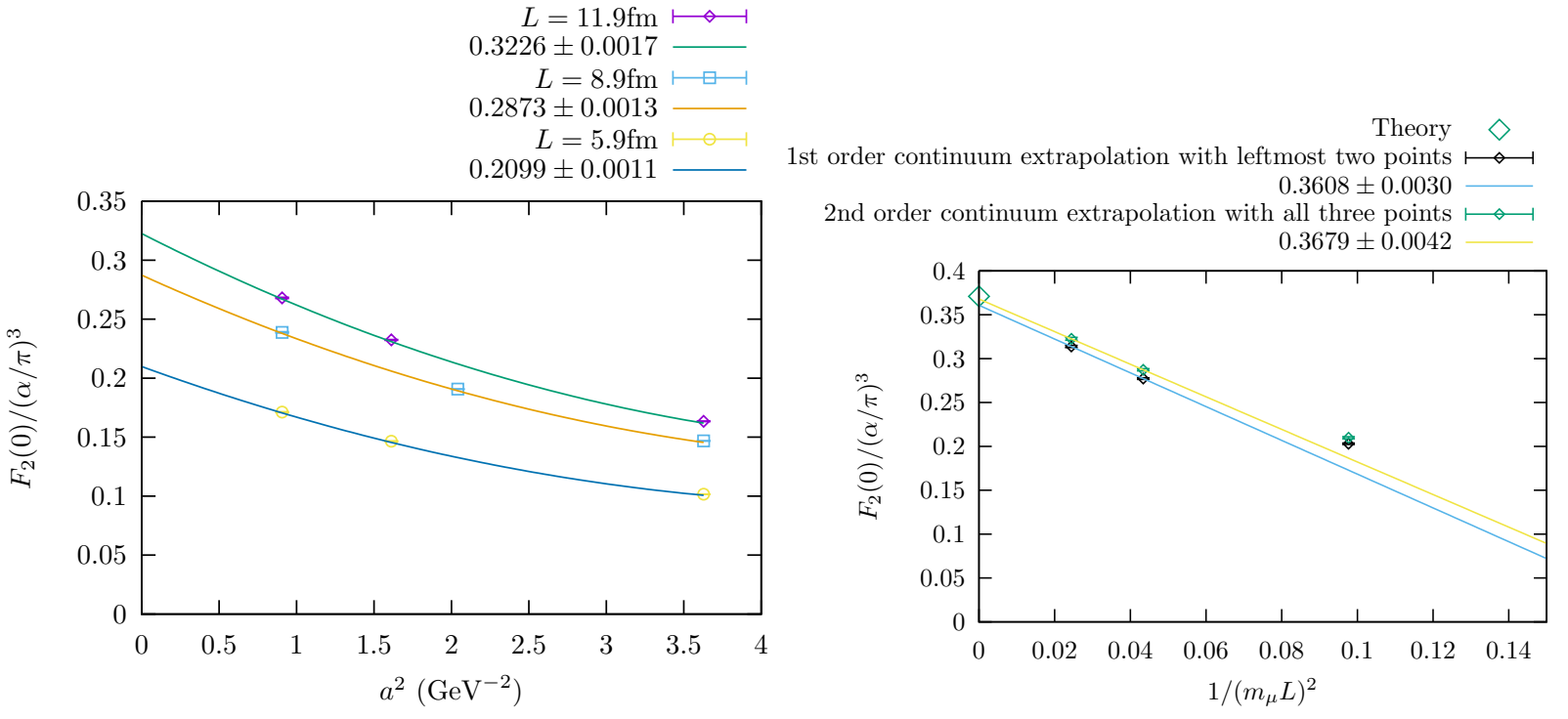

Figure 14. **Pure QED computation**. Muon leptonic light by light contribution to muon $g-2$. Phys.Rev. D93 (2016) 1, 014503. arXiv:1510.07100.

- $\mathcal{O}(1/L^2)$ finite volume effect, because the photons are emitted from a conserved loop.

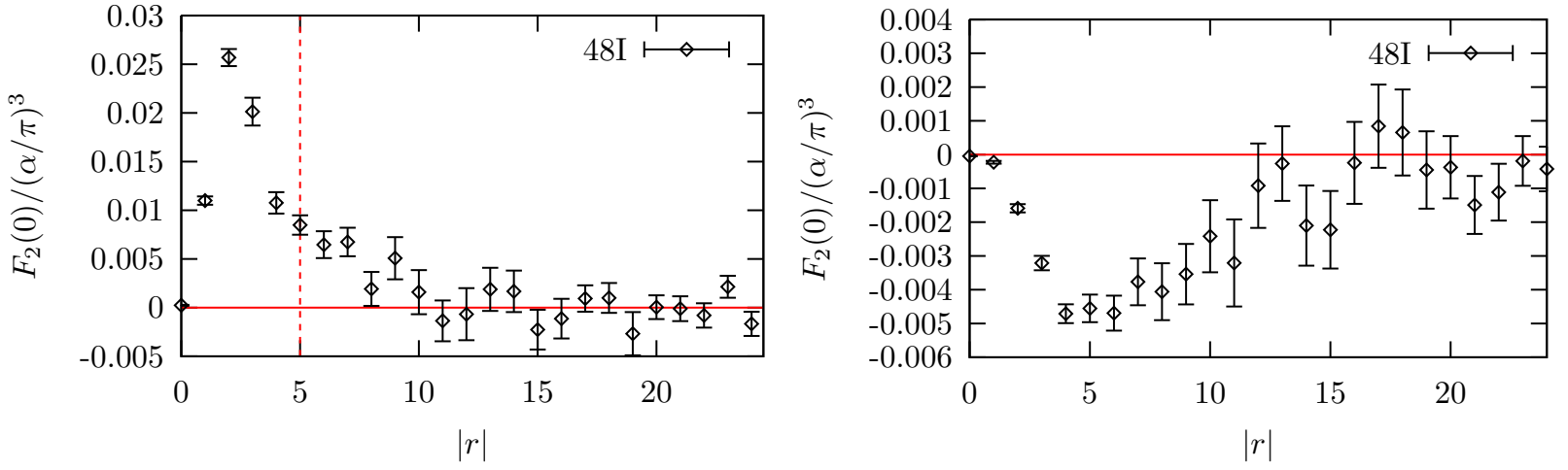

Figure 15. $48^3 \times 96$ lattice, with $a^{-1} = 1.73\text{GeV}$, $m_\pi = 139\text{MeV}$, $m_\mu = 106\text{MeV}$. Left: connected diagrams contribution. Right: leading disconnected diagrams contribution.

- We use Lanczos, AMA, and zMobius techniques to speed up the computations.
- 65 configurations are used. They each are separated by 20 MD time units.

$$\left.\frac{g_\mu - 2}{2}\right|_{\text{cHLbL}} = (0.0926 \pm 0.0077) \times \left(\frac{\alpha}{\pi}\right)^3 = (11.60 \pm 0.96) \times 10^{-10} \quad (17)$$

$$\left.\frac{g_\mu - 2}{2}\right|_{\text{dHLbL}} = (-0.0498 \pm 0.0064) \times \left(\frac{\alpha}{\pi}\right)^3 = (-6.25 \pm 0.80) \times 10^{-10} \quad (18)$$

$$\left.\frac{g_\mu - 2}{2}\right|_{\text{HLbL}} = (0.0427 \pm 0.0108) \times \left(\frac{\alpha}{\pi}\right)^3 = (5.35 \pm 1.35) \times 10^{-10} \quad (19)$$

Outline

- Muon Anomalous Magnetic Moment
- BNL E821 (0.54 ppm) and Standard Model Prediction
- Point Source Photon Method
- Simulations
  - $\rightarrow$ Muon Leptonic Light by Light
  - $\rightarrow$ $139\mathrm{MeV}$ Pion $48^3 \times 96$ Lattice
- **Finite Volume Effects - QCD box inside QED box**
- Long Distance Contribution
- Conclusions and Future Plans

$$\frac{F_2^{\mathrm{cHLbL}}(q^2=0)}{m}\frac{(\sigma_{s',s})_i}{2} = \sum_{r,\tilde{z}} \mathfrak{Z}\left(\frac{r}{2},-\frac{r}{2},\tilde{z}\right)\sum_{\tilde{x}_{\mathrm{op}}}\frac{1}{2}\epsilon_{i,j,k}(\tilde{x}_{\mathrm{op}})_j \cdot i\,\bar{u}_{s'}(\vec{0})\,\mathcal{F}_k^C\left(\frac{r}{2},-\frac{r}{2},\tilde{z},\tilde{x}_{\mathrm{op}}\right)u_s(\vec{0}) \tag{20}$$

$$\mathcal{F}_\nu^C(x,y,z,x_{\mathrm{op}}) = (-ie)^6\,\mathcal{G}_{\rho,\sigma,\kappa}(x,y,z)\sum_{q=u,d,s}(e_q/e)^4 \tag{21}$$

$$\times\ \frac{1}{3}\left\langle \mathrm{tr}\left[-\gamma_\rho S_q(x,z)\gamma_\kappa S_q(z,y)\gamma_\sigma S_q(y,x_{\mathrm{op}})\gamma_\nu S_q(x_{\mathrm{op}},x)\right] + \text{other 2 permutations}\right\rangle_{\mathrm{QCD}}$$

- The integrand decreases exponentially if one of r, z, or x_{op} become large. The fact that the sum is limited within the lattice only has exponentially suppressed effect. We have use the moment method to take $q\to 0$ limit, eliminating that part of the "finite volume" effect.
- However, $\mathcal{G}(x,y,z)$ involves massless photon propagators. Thus, evaluating this function in a small volume leads to $\mathcal{O}(1/L^2)$ finite volume effects.
- Solution: do not evaluate $\mathcal{G}(x,y,z)$ within the QCD box. We evaluate it in larger QED boxes. We are also working on numerical strategies to compute the sum in infinite volume. This way, we can capture the major part of the finite volume effects with the QCD lattice just large enough to contain the quark loop.

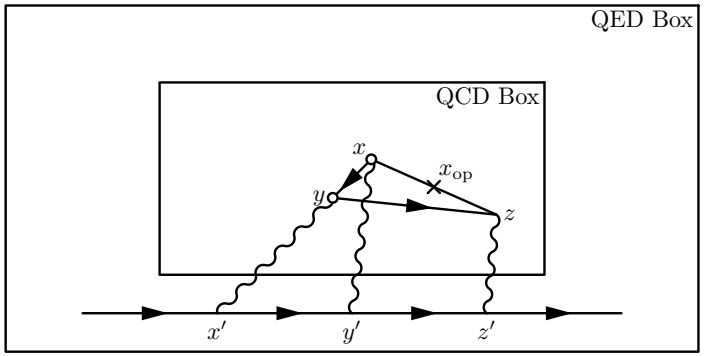

Figure 16. QCD box inside QED box illustration.

$$\mathcal{F}_\nu^C(x,y,z,x_{\rm op}) = (-ie)^6\,\mathcal{G}_{\rho,\sigma,\kappa}(x,y,z)\sum_{q=u,d,s}(e_q/e)^4 \tag{22}$$

$$\times\ \frac{1}{3}\Big\langle \mathrm{tr}\Big[-\gamma_\rho S_q(x,z)\gamma_\kappa S_q(z,y)\gamma_\sigma S_q(y,x_{\rm op})\gamma_\nu S_q(x_{\rm op},x)\Big] + \text{other 2 permutations}\Big\rangle_{\rm QCD}$$

$$\begin{aligned}&\mathcal{G}_{\rho,\sigma,\kappa}(x,y,z) \\ &= e^{m_\mu(t_{\rm snk}-t_{\rm src})}\sum_{x',y',z'} G_{\rho,\rho'}(x,x')G_{\sigma,\sigma'}(y,y')G_{\kappa,\kappa'}(z,z') \\ &\cdot \sum_{\vec{x}_{\rm snk},\vec{x}_{\rm src}} [S_\mu(x_{\rm snk},x')\gamma_{\rho'}S_\mu(x',z')\gamma_{\kappa'}S_\mu(z',y')\gamma_{\sigma'}S_\mu(y',x_{\rm src}) \\ &\quad + S_\mu(x_{\rm snk},z')\gamma_{\kappa'}S_\mu(z',x')\gamma_{\rho'}S_\mu(x',y')\gamma_{\sigma'}S_\mu(y',x_{\rm src}) + \text{other 4 permutations}].\end{aligned} \tag{23}$$

Ensemble	$m_\pi L$	QCD Size	QED Size	$\frac{F_2(q^2=0)}{(\alpha/\pi)^3}$
16I	3.87	$16^3 \times 32$	$16^3 \times 32$	0.1158(8)
24I	5.81	$24^3 \times 64$	$24^3 \times 64$	0.2144(27)
16I-24		$16^3 \times 32$	$24^3 \times 64$	0.1674(22)

Table 2. arXiv:1511.05198. Finite volume effects studies. $a^{-1} = 1.747$ GeV, $m_\pi = 423$ MeV, $m_\mu = 332\,\mathrm{MeV}$.

- Large finite volume effects with these ensembles and muon mass.
- Increasing the QED box size help reducing the finite volume effect, but haven't completely fixed the problem.
- Suggesting significant QCD finite volume effect.
- The histogram plot may help us further investigating this QCD finite volume effect.

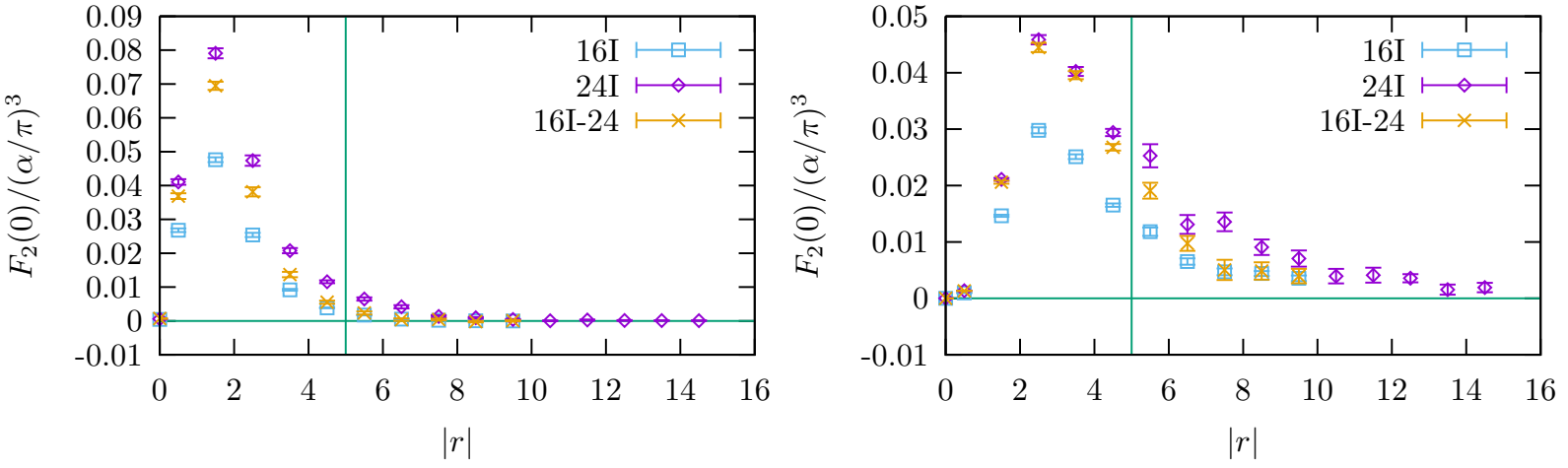

Figure 17. arXiv:1511.05198. Above plots show histograms of the contribution to F_2 from different separations $|r| = |x - y|$. The sum of all these points gives the final result for F_2. The vertical lines at $|r| = 5$ in the plots indicate the value of $r_{\max}$. The left plot is evaluated with z sumed over longer distance region, so the small r region includes most of the contribution. The right plot is evaluated with z sumed over longer distance region, so the QCD finite volume is better controlled in the small r region.

$$\sum_{\substack{z \\ |x-y|<\min(|x-z|,|y-z|)}} \quad \text{v.s.} \quad \sum_{\substack{z \\ |x-y|>\max(|x-z|,|y-z|)}}$$

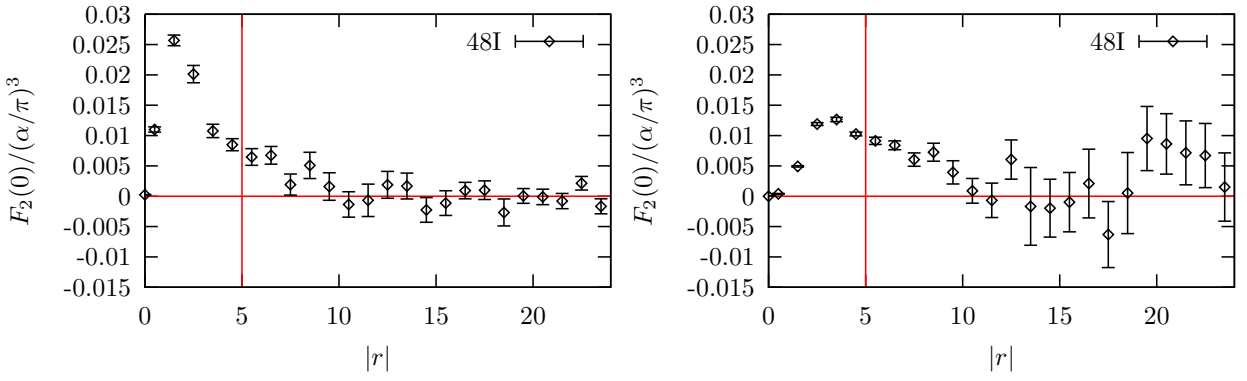

Figure 18. $48^3 \times 96$ lattice, with $a^{-1} = 1.73\text{GeV}$, $m_\pi = 139\text{MeV}$, $m_\mu = 106\text{MeV}$. The left plot is evaluated with z sumed over longer distance region, so the small r region includes most of the contribution. The right plot is evaluated with z sumed over longer distance region, so the QCD finite volume is better controlled in the small r region.

- Contribution vanishes long before reaching the boundary of the lattice.
- Suggesting the QCD finite volume effects be small in this case.
- Simply increasing the QED box will fix most of the finite volume effects.

Outline

- Muon Anomalous Magnetic Moment
- BNL E821 (0.54 ppm) and Standard Model Prediction
- Point Source Photon Method
- Simulations
  - → Muon Leptonic Light by Light
  - → $139\mathrm{MeV}$ Pion $48^3 \times 96$ Lattice
- Finite Volume Effects - QCD box inside QED box
- **Long Distance Contribution**
- Conclusions and Future Plans

Long Distance Contribution - π^0 exchange

When the 4-point function can be viewd as π^0 exchange, and its two ends, a and b, are far separated:

$$\langle \bar{u}\gamma_5 u(a)(\bar{u}\gamma_5 u + \bar{d}\gamma_5 d)(b)\rangle \approx 0 \tag{24}$$

That is

$$\langle \bar{u}\gamma_5 u(a)\bar{d}\gamma_5 d(b)\rangle \approx -\frac{1}{2}\langle \bar{u}\gamma_5 u(a)(\bar{u}\gamma_5 u - \bar{d}\gamma_5 d)(b)\rangle \tag{25}$$

Above is a relation between disconnected diagram π^0 exchange (left hand side) and connected diagram π^0 exchange (right hand side).

Multiplied by appropriate charge factors

$$\text{Connected contribution} \quad \left[\left(\frac{2}{3}\right)^4 + \left(-\frac{1}{3}\right)^4\right] = \frac{17}{81} \tag{26}$$

$$\text{Disconnected contribution} \quad \left[\left(\frac{2}{3}\right)^2 + \left(-\frac{1}{3}\right)^2\right]^2 \left(-\frac{1}{2}\right) = \frac{25}{87}\left(-\frac{1}{2}\right) \tag{27}$$

$$\text{Connected} : \text{Disconnected} = 34 : -25 \tag{28}$$

When the 4 points of the 4-point function are all far separated:

$$\begin{aligned} (e_u^4 + e_d^4)C &\quad \text{Connected diagram contribution} \\ (e_u^2 + e_d^2)^2\, D &\quad \text{Leading order disconnected diagram contribution} \\ (e_u + e_d)\,(e_u^3 + e_d^3)\, D' &\quad \text{Next leading order disconnected diagram contribution} \end{aligned}$$

$$\begin{aligned} \mathcal{M} &\approx (e_u^4 + e_d^4)\, C + (e_u^2 + e_d^2)^2\, D + (e_u + e_d)\,(e_u^3 + e_d^3)\, D' \\ &\propto (e_u - e_d)^4 \end{aligned} \tag{29}$$

$$C : D : D' = -2 : -3 : 4 \tag{30}$$

$$\text{Connected} : \text{LO-disconnected} : \text{NLO-disconnected} = -34 : -75 : 28 \tag{31}$$

Outline

- Muon Anomalous Magnetic Moment
- BNL E821 (0.54 ppm) and Standard Model Prediction
- Point Source Photon Method
- Simulations
  - $\rightarrow$ Muon Leptonic Light by Light
  - $\rightarrow$ $139\mathrm{MeV}$ Pion $48^3 \times 96$ Lattice
- Finite Volume Effects - QCD box inside QED box
- Long Distance Contribution
- **Conclusions and Future Plans**

Conclusions and Future Plans

Using the recently developed methods, we have computed the connected hadronic light-by-light contribution with physical pion mass. We use a $48^3 \times 96$ lattice where $L = 5.5\text{fm}$, $m_\pi = 139\text{MeV}$, $m_\mu = 106\text{MeV}$. 65 configurations are used in the calculation.

$$\left.\frac{g_\mu - 2}{2}\right|_{\text{cHLbL}} = (0.0926 \pm 0.0077)\left(\frac{\alpha}{\pi}\right)^3 = (11.60 \pm 0.96) \times 10^{-10} \tag{32}$$

We have extended the methods to cover the leading disconnected diagrams.

$$\left.\frac{g_\mu - 2}{2}\right|_{\text{dHLbL}} = (-0.0498 \pm 0.0064)\left(\frac{\alpha}{\pi}\right)^3 = (-6.25 \pm 0.80) \times 10^{-10} \tag{33}$$

The sum of these two contributions is:

$$\left.\frac{g_\mu - 2}{2}\right|_{\text{HLbL}} = (0.0427 \pm 0.0108)\left(\frac{\alpha}{\pi}\right)^3 = (5.35 \pm 1.35) \times 10^{-10} \tag{34}$$

- We expect rather large finite volume and finite lattice spacing corrections.
- Most of the finite volume errors come from the QED part of the calcutions. They can be corrected by perform only the QED part of the calculation in a larger or possibly infinite volume.
- The finite lattice spacing errors can be corrected by simply performing the same calculation on a finer $64^3 \times 128$ lattice.

Thank You!

Study the spatial component,

$$\langle \mathbf{p}', s' | i\,\mathbf{j}(\mathbf{x}_{\rm op}=0) | \mathbf{p}, s \rangle \;=\; -e\,\bar{u}_{s'}(\mathbf{p}') \left[F_1(q^2)\, i\,\boldsymbol{\gamma} - \frac{F_2(q^2)}{m}\, i\,\mathbf{q}\times\frac{\boldsymbol{\Sigma}}{2} \right] u_s(\mathbf{p}) \tag{35}$$

$$[\gamma_i, \gamma_j] \;=\; 2\,i\,\epsilon_{ijk}\Sigma_k \tag{36}$$

With Gordon identity

$$\bar{u}_{s'}(\mathbf{p}')\, i\boldsymbol{\gamma}\, u_s(\mathbf{p}) \;=\; \bar{u}_{s'}(\mathbf{p}') \left(\frac{\mathbf{p}'+\mathbf{p}}{2m} - \frac{1}{m}\, i\,\mathbf{q}\times\frac{\boldsymbol{\Sigma}}{2} \right) u_s(\mathbf{p}) \tag{37}$$

$$\begin{aligned} &\langle \mathbf{p}', s' | i\,\mathbf{j}(\mathbf{x}_{\rm op}=0) | \mathbf{p}, s \rangle \\ =\;& -e\,\bar{u}_{s'}(\mathbf{p}') \left[F_1(q^2)\,\frac{\mathbf{p}'+\mathbf{p}}{2m} - \frac{F_1(q^2)+F_2(q^2)}{m}\, i\,\mathbf{q}\times\frac{\boldsymbol{\Sigma}}{2} \right] u_s(\mathbf{p}) \end{aligned} \tag{38}$$

Consider a normalized state

$$|\psi\rangle \;=\; \int \frac{d^3p}{(2\pi)^3}|\mathbf{p},s\rangle\psi_s(\mathbf{p}) \tag{39}$$

We require the state with the momentum almost zero and the expectation value of the current exactly zero:

$$\int d^3x_{\rm op}\langle\psi|i\,\mathbf{j}(\mathbf{x}_{\rm op})|\psi\rangle \;=\; 0 \tag{40}$$

We then consider the following amplitude with extremely small $\mathbf{q}\ll\Delta\mathbf{p}\sim 1/\Delta\mathbf{x}$.

$$\mathcal{M} \;=\; \int d^3x_{\rm op}\exp(i\,\mathbf{q}\cdot\mathbf{x}_{\rm op})\langle\psi|i\,\mathbf{j}(\mathbf{x}_{\rm op})|\psi\rangle \tag{41}$$

We can safely subtract zero

$$\begin{aligned}\mathcal{M} \;&=\; \int d^3x_{\rm op}\,[\exp(i\,\mathbf{q}\cdot\mathbf{x}_{\rm op})-1]\langle\psi|i\,\mathbf{j}(\mathbf{x}_{\rm op})|\psi\rangle \\ &\approx\; \int d^3x_{\rm op}\,i\,\mathbf{q}\cdot\mathbf{x}_{\rm op}\,\langle\psi|i\,\mathbf{j}(\mathbf{x}_{\rm op})|\psi\rangle\end{aligned} \tag{42}$$

On the other hand, with momentum conservation

$$\begin{aligned}\mathcal{M} &= -e\int \frac{d^3p}{(2\pi)^3}\,\psi^*_{s'}(\mathbf{p}+\mathbf{q}/2)\psi_s(\mathbf{p}-\mathbf{q}/2)\\ &\cdot\ \bar{u}_{s'}(\mathbf{p}+\mathbf{q}/2)\left[F_1(q^2)\,\frac{\mathbf{p}}{m}-\frac{F_1(q^2)+F_2(q^2)}{m}\,i\,\mathbf{q}\times\frac{\mathbf{\Sigma}}{2}\right]u_s(\mathbf{p}-\mathbf{q}/2)\end{aligned}\tag{43}$$

The second term is explicitly $\mathcal{O}(\mathbf{q})$, the first term must be at most $\mathcal{O}(\mathbf{q})$ as well. The magnetic moment of a fermion could result from its orbital angular momentum even if its momentum is small, because of large size. One way we can eliminate that is to require $\psi^*_s(\mathbf{p})=\psi_s(\mathbf{p})$, so that the $\mathcal{O}(\mathbf{q})$ part of the first term vanishes. Only keep the leading $\mathcal{O}(\mathbf{q})$ term, we obtain

$$\mathcal{M} \approx e\,\frac{F_1(q^2=0)+F_2(q^2=0)}{m}\,i\,\mathbf{q}\times\left\langle\frac{\mathbf{\Sigma}}{2}\right\rangle\tag{44}$$

$$\left\langle\frac{\mathbf{\Sigma}}{2}\right\rangle = \int\frac{d^3p}{(2\pi)^3}\psi^*_{s'}(\mathbf{p})\psi_s(\mathbf{p})\bar{u}_{s'}(\mathbf{p})\frac{\mathbf{\Sigma}}{2}u_s(\mathbf{p})\tag{45}$$

Combine the results from previous two approaches:

$$e\,\frac{F_1(q^2=0)+F_2(q^2=0)}{m}\,i\,\mathbf{q}\times\left\langle\frac{\boldsymbol{\Sigma}}{2}\right\rangle \;\approx\; \int d^3x_{\rm op}\,i\,\mathbf{q}\cdot\mathbf{x}_{\rm op}\,\langle\psi|i\,\mathbf{j}(\mathbf{x}_{\rm op})|\psi\rangle \tag{46}$$

Cancel the $\mathbf{q}$, we obtain

$$e\,\frac{F_1(q^2=0)+F_2(q^2=0)}{m}\,\epsilon_{ijk}\left\langle\frac{\Sigma_k}{2}\right\rangle \;=\; \int d^3x_{\rm op}\,(x_{\rm op})_j\,\langle\psi|i\,j_i(\mathbf{x}_{\rm op})|\psi\rangle \tag{47}$$

Finally

$$-e\,\frac{F_1(q^2=0)+F_2(q^2=0)}{m}\left\langle\frac{\boldsymbol{\Sigma}}{2}\right\rangle \;=\; \left\langle\psi\left|\int\frac{1}{2}\,\mathbf{x}_{\rm op}\times i\,\mathbf{j}(\mathbf{x}_{\rm op})\,d^3x_{\rm op}\right|\psi\right\rangle \tag{48}$$

Summing Over x_{op}

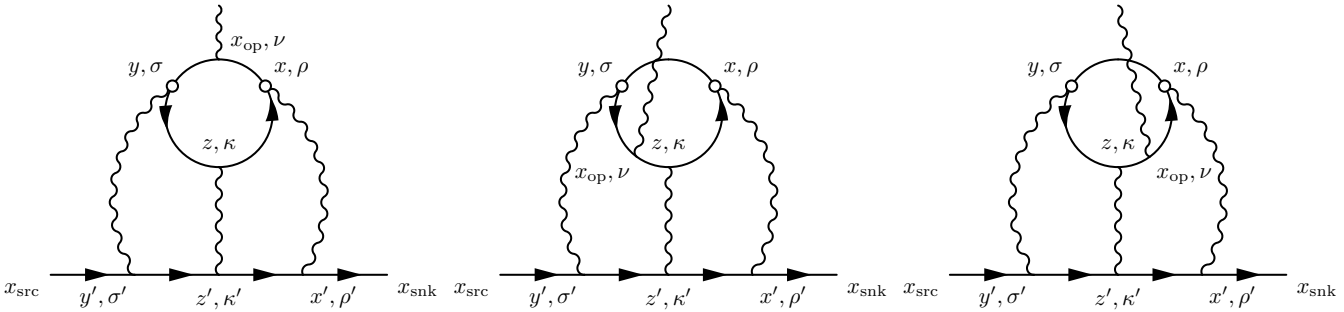

Figure 19. All three different possible insertions for the external photon. 5 other possible permutations of the three internal photons are not shown.

$$\mathcal{M}_\nu^{\mathrm{LbL}}(\mathbf{q}) = \exp(i\,\mathbf{q}\cdot\mathbf{x}_{\mathrm{op}})\,\mathcal{M}_\nu^{\mathrm{LbL}}(\mathbf{q};x_{\mathrm{op}}) \tag{49}$$

$$= \sum_{x,y}\left[\sum_z \exp(i\,\mathbf{q}\cdot\mathbf{x}_{\mathrm{op}})\,\mathcal{F}_\nu(\mathbf{q};x,y,z,x_{\mathrm{op}})\right] \tag{50}$$

$$= \sum_{x,y}\sum_z \exp\Big(i\,\mathbf{q}\cdot\Big(\mathbf{x}_{\mathrm{op}} - \frac{\mathbf{x}+\mathbf{y}}{2}\Big)\Big)$$

$$\cdot\ \mathcal{F}_\nu\Big(\mathbf{q};\frac{x-y}{2},-\frac{x-y}{2},z-\frac{x+y}{2},x_{\mathrm{op}}-\frac{x+y}{2}\Big) \tag{51}$$

$$= \sum_r\left[\sum_{z,x_{\mathrm{op}}} \exp(i\,\mathbf{q}\cdot\mathbf{x}_{\mathrm{op}})\,\mathcal{F}_\nu\Big(\mathbf{q};-\frac{r}{2},+\frac{r}{2},z,x_{\mathrm{op}}\Big)\right] \tag{52}$$

In the second last step, we use the translational covariance of $\mathcal{F}$.

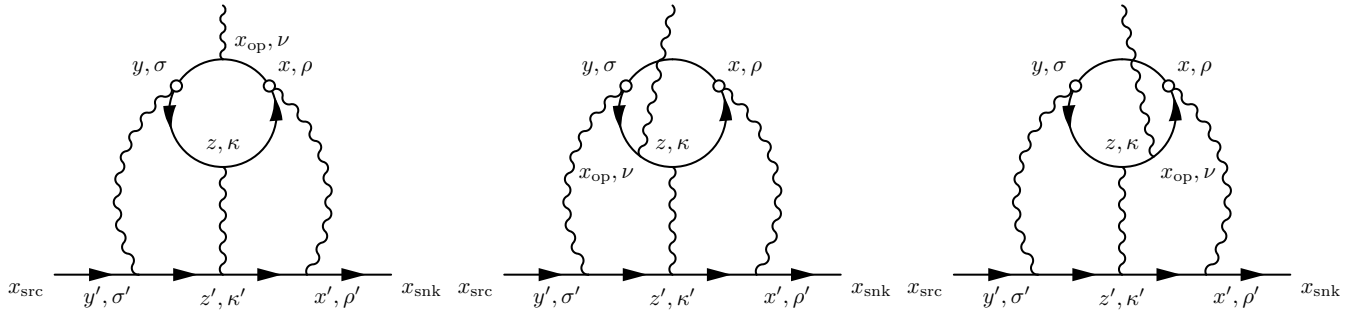

Figure 20. All three different possible insertions for the external photon. 5 other possible permutations of the three internal photons are not shown.

$$\mathcal{M}_\nu^{\rm LbL}(\mathbf{q}) = \sum_r \left[\sum_{z,x_{\rm op}} \exp(i\,\mathbf{q}\cdot\mathbf{x}_{\rm op})\,\mathcal{F}_\nu\Big(\mathbf{q}; -\frac{r}{2}, +\frac{r}{2}, z, x_{\rm op}\Big) \right] \tag{53}$$

$$= \sum_r \left[\sum_{z,x_{\rm op}} (1 + i\,\mathbf{q}\cdot\mathbf{x}_{\rm op})\,\mathcal{F}_\nu\Big(\mathbf{q}; -\frac{r}{2}, +\frac{r}{2}, z, x_{\rm op}\Big) \right] \tag{54}$$

$$= \sum_r \left[\sum_{z,x_{\rm op}} i\,\mathbf{q}\cdot\mathbf{x}_{\rm op}\,\mathcal{F}_\nu\Big(\mathbf{q}; -\frac{r}{2}, +\frac{r}{2}, z, x_{\rm op}\Big) \right] \tag{55}$$

- In the second last step we can drop the "1" term because of current conservation for the quark loop.

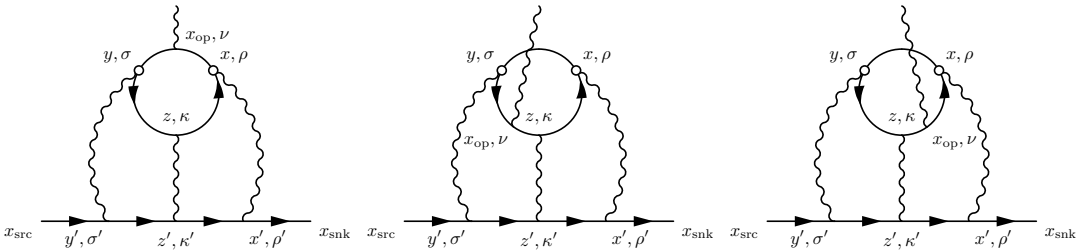

Figure 21. All three different possible insertions for the external photon. 5 other possible permutations of the three internal photons are not shown.

$$\bar{u}_{s'}(\mathbf{q}/2)\mathcal{M}_{\nu}^{\rm LbL}(\mathbf{q})u_s(-\mathbf{q}/2) \;=\; \bar{u}_{s'}(\mathbf{q}/2)\left(i\frac{F_2(q^2)}{4m}[\gamma_\nu,\gamma_\rho]q_\rho\right)u_s(-\mathbf{q}/2) \tag{56}$$

$$\mathcal{M}_{\nu}^{\rm LbL}(\mathbf{q}) \;=\; \sum_r\left[\sum_{z,x_{\rm op}} i\mathbf{q}\cdot\mathbf{x}_{\rm op}\,\mathcal{F}_\nu\left(\mathbf{q};-\frac{r}{2},+\frac{r}{2},z,x_{\rm op}\right)\right] \tag{57}$$

Taking $q\to 0$ limit by computing derivative with respect to q, we obtained the familiar magnetic moment formula.

$$\begin{aligned}&\frac{F_2(0)}{m}\,\bar{u}_{s'}(\mathbf{0})\frac{\vec{\Sigma}}{2}u_s(\mathbf{0})\\ =\;&\sum_r\left[\sum_{z,x_{\rm op}}\frac{1}{2}\,\vec{x}_{\rm op}\times\bar{u}_{s'}(\mathbf{0})\,i\vec{\mathcal{F}}\left(\mathbf{0};x=-\frac{r}{2},y=+\frac{r}{2},z,x_{\rm op}\right)u_s(\mathbf{0})\right]\end{aligned} \tag{58}$$